

# Development of Wound Healing Scaffold Using ZnO and TiO<sub>2</sub> Nanoparticles

Younes Beygi-Khosrowshahi\*, Fatemeh Samadian

Department of Chemical Engineering, Azarbaijan Shahid Madani University, Tabriz, Iran

## Research Article

**Received:** 15-Feb-2024, Manuscript No. JOMS-24-127667; **Editor assigned:** 19-Feb-2024, PreQC No. JOMS-24-127667 (PQ); **Reviewed:** 04-Mar-2024, QC No. JOMS-24-127667; **Revised:** 11-Mar-2024, Manuscript No. JOMS-24-127667 (R); **Published:** 18-Mar-2024, DOI: 10.4172/2321-6212.12.1.003

**\*For Correspondence:**  
Younes Beygi-Khosrowshahi,  
Department of Chemical Engineering,  
Azarbaijan Shahid Madani University,  
Tabriz, Iran

**E-mail:** yonesbeygi@gmail.com

**Citation:** Khosrowshahi YB, et al. Development of Wound Healing Scaffold Using ZnO and TiO<sub>2</sub> Nanoparticles. RRJ Mater Sci. 2024;12:003.

**Copyright:** © 2024 Khosrowshahi YB, et al. This is an open-access article distributed under the terms of the Creative Commons Attribution License, which permits unrestricted use, distribution, and reproduction in any medium, provided the original author and source are credited.

**Copyright:** © 2024 Khosrowshahi YB, et al. This is an open-access article distributed under the terms of the Creative Commons Attribution License, which permits unrestricted use, distribution, and reproduction in any medium, provided the original author and source are credited.

**Copyright:** © 2024 Khosrowshahi YB, et al. This is an open-access article distributed under the terms of the Creative Commons Attribution License, which permits unrestricted use, distribution, and reproduction in any medium, provided the original author and source are credited.

## ABSTRACT

The goal of this experiment is to produce a nanocomposite porous scaffold, using an electrospinning method that has biological properties to use as a skin Tissue Engineering (TE) and wound dressing. Polyhydroxyethyl methacrylate (PHEMA), Polycaprolactone (PCL), Titanium Oxide (TiO<sub>2</sub>) nanoparticles, and Zinc Oxide (ZnO) nanoparticles, used to fabricate this scaffold. After the polymers were synthesized, both polymers were dissolved in chloroform, and nanoparticles were added. The diameter of the fibers obtained depends on the amount of addition of each nanoparticle, the injection rate of the device and the voltage, and the distance between the collector and the needle. Scanning Electron Microscopy (SEM) images showed the morphology of the scaffold and the cells can adhere well to nanofibers. The mechanical property test showed appropriate mechanical properties for this polymeric scaffold. X-Ray Diffraction Pattern (XRD) and Fourier Transform Infrared Spectroscopy (FTIR) results confirm the successful loading of nanoparticles into the polymer scaffold. Other biological features are characterized with, *in vivo* assay and MTT and antibacterial assay. The results show that this scaffold is suitable to use as a skin tissue scaffold and wound dress.

**Keywords:** Electrospinning; Scaffold; Wound; Zinc oxide; Titanium oxide

## INTRODUCTION

The skin is the body's most important barrier against microorganisms and harmful substances. This barrier works best when healthy. Skin wounds can become infected and bacteria on the surface of the skin enter the body's bloodstream. Nowadays tissue engineering products promising for the treatment of skin lesions such as wounds and deep burns.

Tissue engineering tries to restore the biological activities of damaged tissue to its original state by creating artificial tissue, and therefore plays a key role in wound healing and tissue replacement. Interactions between biomaterials and tissues are highly dependent on the external surface structure of these substitutes. In this regard, the selection of the appropriate scaffold and cell plays a decisive role in achieving skin tissues that have similar characteristics in terms of histology and physiology to normal skin.

Tissue engineering employs engineering and biological science principles and methods for the production and development of biological alternative scaffolds, cells, growth factors and the main components of tissue engineering include polymers. The scaffold is a three-dimensional structure that is used as a framework to guide cells and it is a replacement for the extracellular matrix [1]. The structure of the scaffold must be possible for cells to adhere to it and it should be porous so when implanted on the body, the veins penetrate the scaffold and can feed the cells. One of the main characteristics of scaffolding is its degradability. The scaffold is gradually destroyed after the tissue is formed.

Polymers are usually the best materials for tissue scaffolds than ceramics because polymers have better plasticity. Among different polymers, polycaprolactone has excellent mechanical properties including good biodegradability, low anti-genius, simple process ability, non-toxic products resulting from its destruction.

Biodegradable electro spun PCL nanofibers, due to their advantages such as high surface to volume ratio in comparison with traditional scaffolds, are increasingly used for tissue engineering. Another material that is used in this article is poly hydroxyethyl methacrylate that is a nontoxic sterile polymer composed of 2-hydroxy ethyl methacrylate monomeric units. PHEMA has a hydrophobic structure and hydrophilic cells are unable to adhere to the polymer surface. The cells are non-stick and suspended in 3D space between the environment and the polymer [2]. PHEMA has high solubility in organic solvents such as methanol and ethanol [3]. Furthermore, good mechanical stability, high biocompatibility, and physiological properties make HEMA very useful used in biomedicine.

Recently, nanomaterials have been widely used in many fields due to the development and growth of nanotechnology. Zinc oxide and titanium oxide nanoparticles due to their anti-cancer, anti-bacterial, anti-inflammatory, and binding properties, are used in many fields like drug delivery, food additives, and tissue engineering. Zinc oxide has received much attention due to its unique surface and chemical properties and various functions in ultraviolet emitters, chemical sensors and piezoelectric devices, etc. Moreover, Titanium oxide, due to its special properties, has an amazing ability to destroy the walls of prokaryotes, such as *Escherichia coli* [4,5].

In recent years, electrospinning with the ability to create polymeric nanofibers similar to the extracellular fibrous structure has attracted a lot of attraction. Electro spun nanofibers have many different applications in the fields of tissue engineering, energy storage, filtration, drug release, etc [6-11]. Combining nanoparticles and adding them to a polymer solution and electrospinning this solution and obtaining nanofibers containing nanoparticles is an up-to-date and interesting research field [12].

The diameter of the fibers obtained from the electrospinning process may vary from ten nanometers to several micrometers. Polymeric or composite solutions and high voltage sources are used to prepare electro spun nanofibers [13,14]. One of the advantages of producing nanofibers by electro spin method is that the direction and size of the fibers can be controlled and also the rate and speed of fiber production can be controlled [15].

Simulation of the extracellular matrix fibrous arrangement in the body, high surface to volume ratio, and significant porosity are the most important benefits of electrospinning. Parameters such as polymer molecular weight, concentration, surface tension, viscosity and conductivity of polymer solution, voltage, injection rate, spinner and collector type, and environmental conditions control the electrospinning process [16].

In this research, by using the conventional and inexpensive electrospinning method with using biodegradable and biocompatible polymers like Polycaprolactone (PCL) and Polyhydroxy Ethyl Methacrylate (PHEMA) and ceramic nanoparticles such as TiO<sub>2</sub> and ZnO, we tried to investigate the effect of the composite of these materials on the recovery time and absence of germs and infection at the wound site.

### MATERIALS AND METHODS

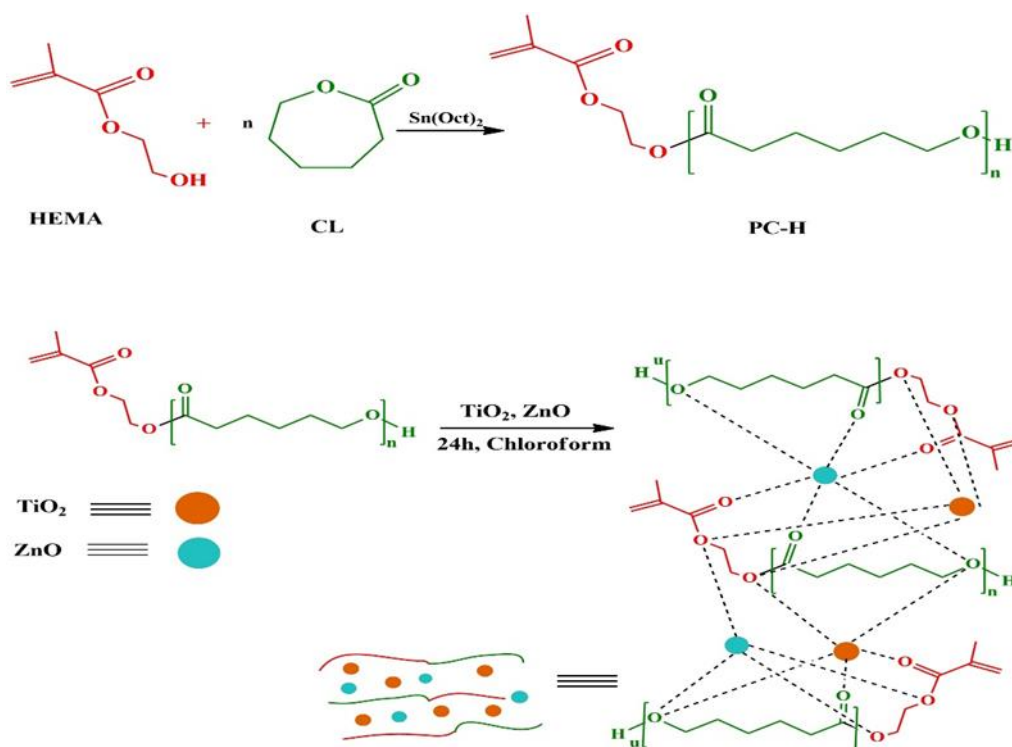
#### Materials used in this experiment

TiO<sub>2</sub>(MW=79.866) and ZnO(MW=81.40) nanoparticles, PCL(Mw=80 KDa), PHEMA(MW=-KDa), phosphate buffer saline(PBS, PH=7.4), Roswell Park Memorial Institute Medium(RPMI medium), Fetal Bovine Serum(FBS, Gibco company), 3(4,5 dimethylthiazol-2yl)-2,5 diphenyltetrazolium bromide(MTT), Ketamine, 70% ethanol solution.

#### Polymer synthesis

The p-H was synthesized by CL, HEMA, and nanoparticles (TiO<sub>2</sub> and ZnO). First, Sn(Oct)<sub>2</sub> (30 mg, 0.074 mmol) was mixed with HEMA (3.8 g, 0.029 mol) in a round-bottom flask at room temperature until Sn(Oct)<sub>2</sub> is completely dissolved. Then, CL(10 g, 0.0877 mol) was heated up to 130°C in a stirred round-bottom flask. The HEMA/Sn(Oct)<sub>2</sub> solution was then added to the flask, and the reaction was carried out for 2 h. The synthesis and nanoparticle loading procedure was shown in Figure 1.

Figure 1. The synthesis of pHEMA/PCL loaded by nano particles.



### **Fiber preparation**

The precursor solutions for electrospinning were prepared in a two-stage approach. First, a suspension of inorganic powder in the solvent mixture was achieved by dispersing 0.5 g of solid in 10 ml of chloroform, all being ultra sonicated for 5 min at 50% amplitude.

Then, 1.6 g of polymer was dissolved in the previously prepared suspension, which led to a final solution with 16% PCL and 5% inorganic powder; this was maintained under magnetic stirring for 24 h for PCL solubilization and general homogenization.

### **Electrospinning process**

The obtained solution was injected into a 5 ml plastic syringe with a metallic needle and subjected to the electrospinning process. In this process electrical field was 19 kv, the feeding rate was 0.5 ml/h and the distance from needle to collector was 18 cm.

### **SEM characterization**

To determine the characteristics of electrospun scaffolds, Scanning Electron Microscopy (SEM) has used. To increase electrical conductivity, the surface of the scaffold was first covered with a thin coating with a thin layer of gold. The device used in this test is manufactured by Philips Netherlands and the model of the microscope is XL30.

### **XRD characterization**

Another analysis used to study the phase composition and crystallization of scaffolding is X-Ray ((XRD) Philips TW 3710) diffraction X-ray diffraction analysis (XRD) has been used to investigate the composition of atoms in the structure of polymer crystals. After reviewing the results obtained from X-ray diffraction analysis, it can be seen that the nanoparticles are loaded into the structure of polymer fibers.

### **FTIR characterization**

To comment on the loading of nanoparticles into polymer fibers and their reaction with polymer functional groups and to identify the functional groups present in the sample, a device Nicolet nexus 670 at a wavelength of 400-30000  $\text{cm}^{-1}$  has been used.

### **Contact angle test**

Goniometer model CA-500A is used to measure the wettability of polymer nanofibers and the contact angle measurement model was sessile drop method. Distilled water is carefully poured on dry samples and in different cases, the contact angle is measured and photographed. The measurement is repeated several times for greater reliability and the contact angle is recorded when the error of the two data is less than 5%.

### **Mechanical properties**

In addition to factors such as biocompatibility and porosity and biodegradability, mechanical properties are also the main features of a suitable scaffold. For this test, a 3\*8 cm sample was used. Tension and strain testing device Z 010, Zwick/Roell, Ulm, Germany, has been used.

### Bio-degradability assay

To evaluate the stability of polymeric scaffolds and measuring the rate of destruction in the body environment, hydrolytic and enzymatic biodegradability test was used. Therefore, the scaffolds were weighed (dry weight) and placed in a phosphate-buffered saline solution (PBS) containing 4 mg/ml trypsin enzyme for one month. During 15 days of biodegradability testing, each week the scaffolds were dried in a freeze dryer and their dry weight was measured. It should be noted that the scaffolding medium was changed weekly and by the end of the fourth week, the remaining mass percentage of the scaffolds was obtained from the following equation. The test was repeated three times for each sample to obtain the mean and standard deviation.

$$\text{Weight lost (\%)} = \frac{W_i - W_f}{W_i} \times 100$$

Where,

$W_i$  is the weight of nanoparticle loaded scaffold in dry state and  $W_f$  is the final wet weight.

### Biocompatibility analysis

**Cell culture:** Skin fibroblast cells were cultured in a tissue culture flask and containing RPMI (cell culture media), 1% antibiotic, and 10% FBS, then incubated at 37 °C, 5% CO<sub>2</sub> and 90% humidity. During this experiment, cell culture media was changed every 2 days.

**Cell viability assay:** This experiment is conducted in both direct and indirect ways. For analysis of proliferation and viability of cells,  $4 \times 10^4$  cells (mouse fibroblast cells, CRL-2017) were seeded in 24 well plates in the presence of sterilized fibrous scaffold, and then RPMI media was added and 48 hours stayed at CO<sub>2</sub> incubator under 90% air condition and 5% CO<sub>2</sub> at 37 °C. After 48 h, the MTT solution was added into each well and kept in dark condition inside of the CO<sub>2</sub> incubator. After spending 8 h, DMSO was added to dissolve formazan crystals. UV spectrometer at a wavelength of 570 nm was used to measure absorbance.

**Cell adhesion assay:** For measuring cell attachment, scaffolds (sterilized scaffold) were put into 6 well plates then  $4 \times 10^4$  cells per well and media was added in each well. The sample was incubated for 8 hours and then the media was changed with new RPMI media. In this step, the sample was washed with PBS solution and glutaraldehyde was used as a fixator.

After that fixator was removed, samples were washed with deionized water. The attached cells were observed with electron scanning microscopy (SEM). There may be three modes in the interaction between the cell and the polymer scaffold [17,18].

In the first type, the interaction between the cell and the polymer scaffold is non-adhesive, in other words, no interaction occurs and in the second type, the cells interact with each other but can easily separate. This type of adhesion is called inactive adhesion. In the second type, the surface response is controlled by physicochemical interactions between the polymer surface, adsorbed proteins, and adhesive cells [19,20]. In the third type, the cells interact spontaneously and strongly and adhere firmly to the surface of the polymer.

### Antibacterial properties

As mentioned earlier, TiO<sub>2</sub> and ZnO nanoparticles have antibacterial properties that can be examined using gram-negative and gram-positive bacteria due to agar diffusion. For this test *Escherichia coli* (*E.coli*) from the Enterobacteriaceae family as gram-negative bacteria and *Staphylococcus aureus* from Staphylococcaceae family as gram-positive bacteria are used. The diameter of the circular scaffolds is one centimeter and we test the scaffolds with 2.5% and a scaffold without nanoparticles.

Nutrient agar media was poured into a bacterial culture plate and after that media dried, bacteria cultured on this. Then we place the samples on the plate and after that plate was kept in an incubator at 37 °C for 24 h. Lack of bacterial growth around the samples is evident that has shown in pictures.

### In vivo experiment

In terms of the number of animals used in biomedical research, the rat is regarded as the second laboratory animal. These mice are easily adapted to research methods. Today's laboratory rats are domesticated genera of *Rattus norvegicus*. In clinical trials, all tests were confirmed by the Faculty of Veterinary Medicine of Tabriz University.

The animals used for this experiment were four adult rats weighing 283-328 g obtained from the animal experiment center of Tabriz University. Experimental and biodiversity standards have been observed in all stages of surgery and experiments performed on live animals [21,22].

**The rats were kept under this standard condition:** The rats are kept in Plexiglass cages with lattice metal caps and with dimensions of (24\*15\*35). In the cages, the ventilation operation was going well and the cages were cleaned every day.

The light period of the animals was carefully regulated. For example, 14 hours of lighting and 10 hours of darkness.

The temperature of the animals was also kept at standard temperature (25 ± 2 °C). Animal feeding was free and pelleted feed was used. The animal's water container was made of glass or plastic and the rats always had access to safe and healthy water. The humidity was about 55%. The rats daily consumed an average of 20 grams of food and a cup of water. Rat feed includes carbohydrates, vitamins, minerals and proteins. Megataj Agrovvet private Limited, Nagpur Rat and Mice feed used for daily feeding. Before creating the wound, the desired location for the wound is shaved and after that, the shaved place is disinfected. Ketamine has been used to anesthetize the animals that the dose of ketamine is 100 mg/kg body weight.

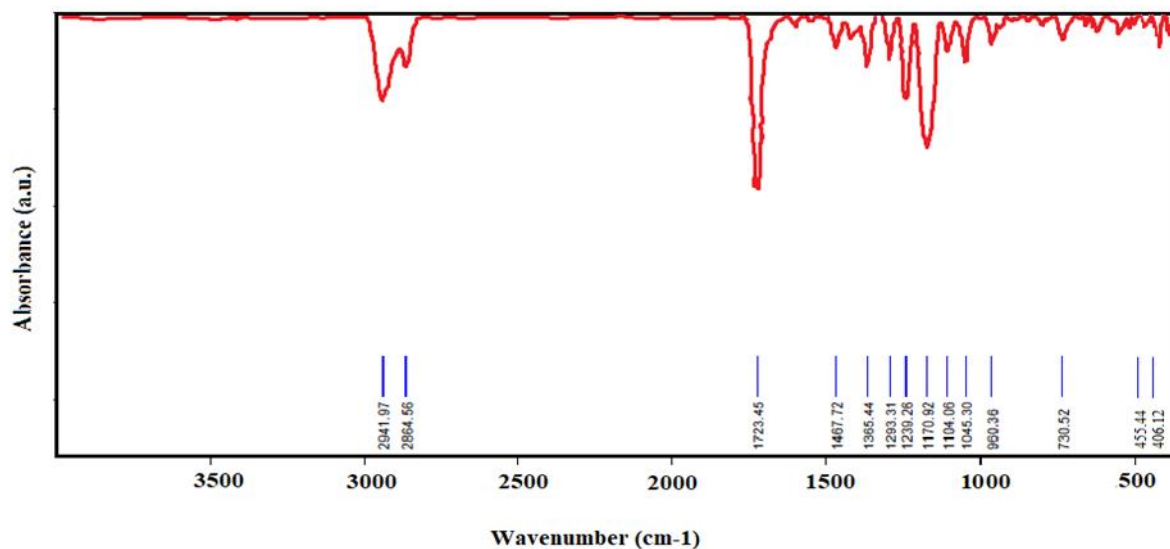
## RESULTS AND DISCUSSION

### FTIR characterization

FT-IR analysis of p-h-t is represented in Figure 2. The absorption bands at 2941 and 2864 cm<sup>-1</sup> are assigned to CH<sub>2</sub> asymmetric stretching and symmetric stretching for PCL and HEMA. The absorption band 1723 cm<sup>-1</sup> is related to the presence of the carbonyl group in PCL. According to Figure 2, due to the interaction of the carbonyl group with metal nanoparticles, the peak intensity of the carbonyl group in PCL has decreased. The absorption bands at 1045,

1104, and 1239  $\text{cm}^{-1}$  are related to the stretching vibrations of the C-O-C (PCL). Bonds containing metal-oxygen are found in lower wavenumbers. Absorption peaks 455 and 406  $\text{cm}^{-1}$  indicate the presence of these bonds in the structure of P-H [23,24]. Also, due to the interaction of the hydroxyl group (HEMA) with PCL of this group in region 3200  $\text{cm}^{-1}$  has been removed as shown in Figure 2.

Figure 2. FT-IR spectra of P-H.



### XRD characterization

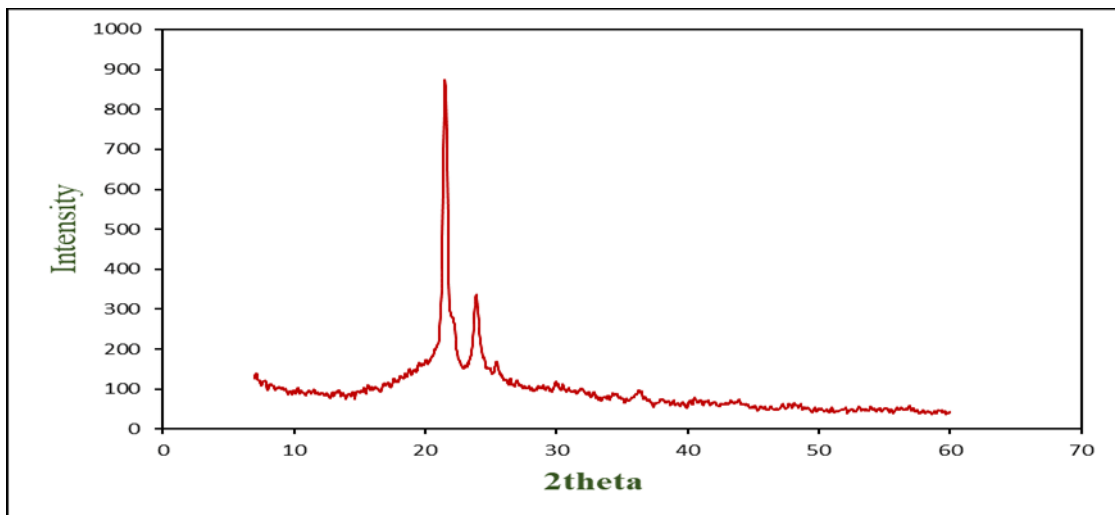
Figure 3 shows the XRD pattern of P-H. According to the XRD spectrum pattern [25-27], the displacement peaks of PCL and HEMA from ( $21.31^\circ$ ,  $23.71^\circ$  and  $33^\circ$  respectively) to ( $21.48^\circ$ ,  $23.84^\circ$ ), also the XRD spectrum pattern shows the removal of the peaks of  $\text{TiO}_2$  ( $25.27^\circ$ ,  $36.91^\circ$ ,  $37.77^\circ$ ,  $38.52^\circ$ ,  $48.01^\circ$ ,  $53.84^\circ$ ,  $55.03^\circ$ ,  $62.07^\circ$ ,  $62.64^\circ$ ) and  $\text{ZnO}$  ( $31.76^\circ$ ,  $34.42^\circ$ ,  $36.25^\circ$ ,  $47.53^\circ$ ,  $56.60^\circ$ ,  $62.86^\circ$ ,  $66.37^\circ$ ,  $67.96^\circ$ ,  $69.1^\circ$ ). By increasing the intensity and displacement peaks of PCL and HEMA, it can be concluded that nanoparticles ( $\text{TiO}_2$  and  $\text{ZnO}$ ) have interacted (interactions between hydrophilic  $\text{TiO}_2$ , polar PCL, and HEMA) with PCL and HEMA. These results confirm the successful loading of nanoparticles in the polymer structure.

### Contact angle test

The contact angle value of p-H is shown in Figure 3. The contact angle value ( $131.64^\circ$ ) indicates the hydrophobic surface of this polymer, which is due to the load of HEMA and mineral nanoparticles ( $\text{TiO}_2$  and  $\text{ZnO}$ ) in the structure of the p-H. The presence of HEMA in the structure of the p-H increases the ( $\text{CH}_2$ ) aliphatic part of the polymer and also the interaction of mineral nanoparticles with the hydroxyl group of HEMA reduces the polarity of this part. For these reasons, it shows the polymer exhibit hydrophobic surfaces as shown in Figure 3.



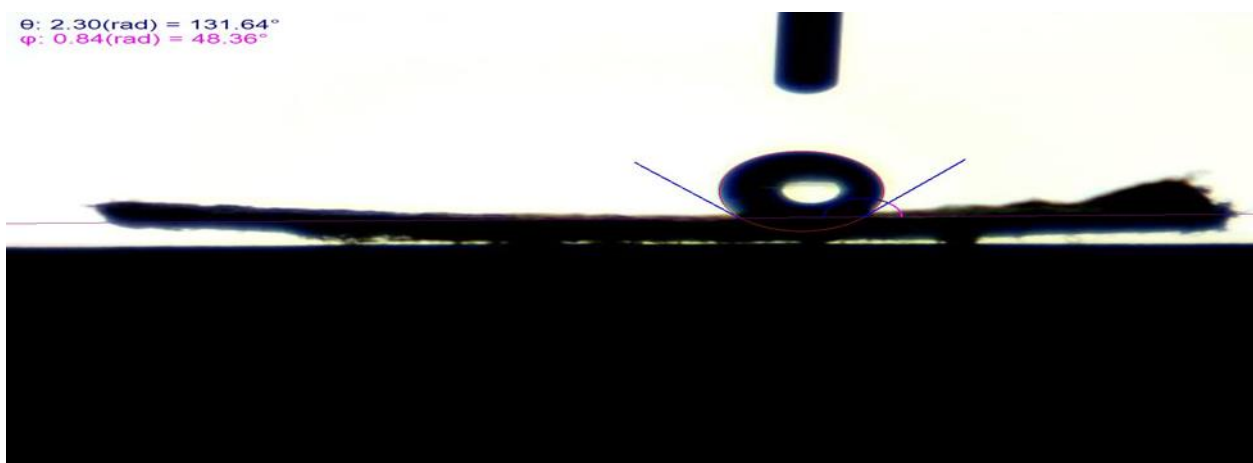
Figure 3. X-ray diagram of a polymer scaffold containing nanoparticles.



### Mechanical properties

The Young modulus or the modulus of elasticity in tension, is a mechanical property that measures the tensile stiffness of a solid material. It quantifies the relationship between tensile stress  $\sigma$  (force per unit area) and axial strain  $\epsilon$  (proportional deformation) in the linear elastic region of a material. The value Young modulus for p-H is 5.18 Mpa. This result shows the appropriate mechanical properties for this polymer as shown in Figure 4.

Figure 4. Schematic of contact test.

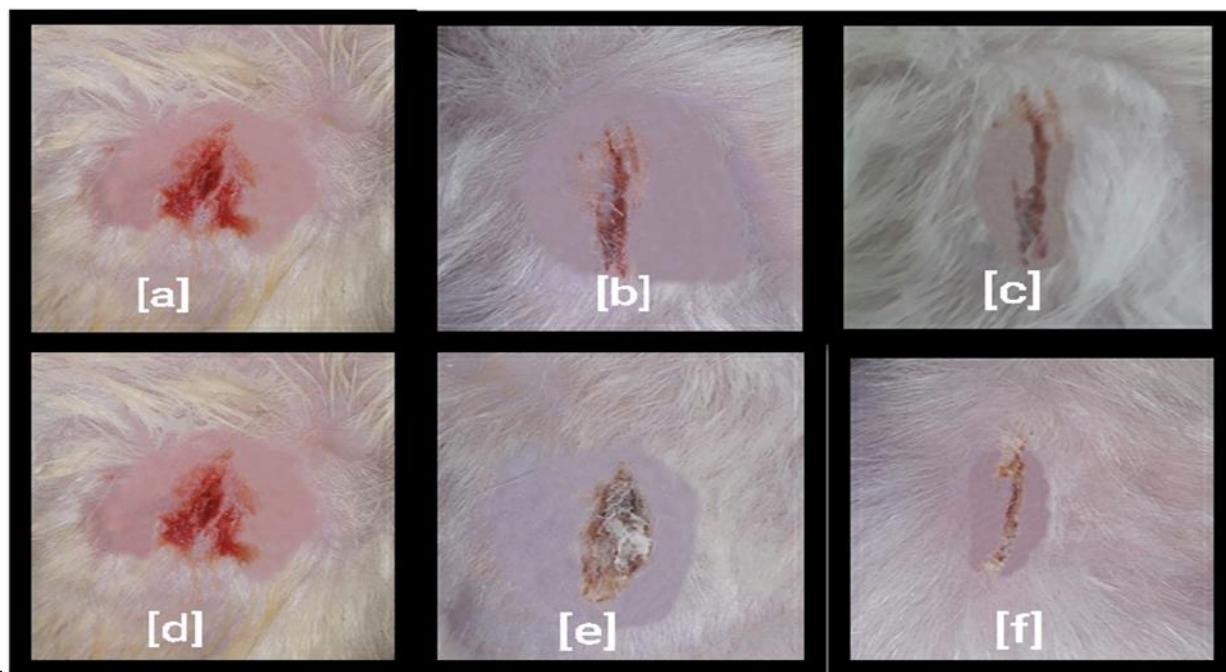


### In vivo experiment

Figure 5 shows how wounds appear in scaffolding and without scaffolding. The wounds were examined on the first, third, and fifth days. Results show that the use of this scaffold due to the use of antibacterial nanoparticles did not cause any inflammatory reactions. Wound area with scaffolding compared with scaffold-free wounds, was less and the wound healing process also happened faster as shown in Figure 5.



**Figure 5.** The figure shows the process of wound healing on different days and conditions with wound dressing and without wound dressing. (a and d) shows the result of examine at first day, all the experimental condition were same; (b) Has no scaffolding and there is evidence of white infection despite the disinfection of wounds and; (c) compared to the wound (f) healed less; (e) A wound that fibrous scaffolding placed on it and it is clear that the scaffold is attached to the surface of the wound; (f) The gaps are very small and it can be said that it has almost completely improved.

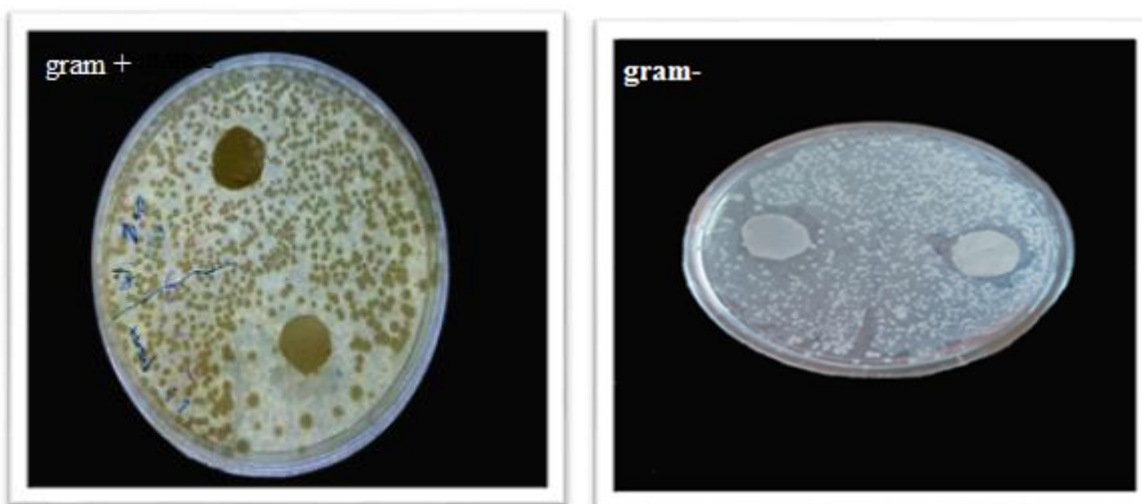


### Investigation of antibacterial behavior of scaffolds

Figure 6 show how wound dressings work against gram-negative and gram-positive bacteria. The results of antibacterial scaffold testing against different types of bacteria, gram-positive and gram-negative bacteria. *Staphylococcus aureus* (ATCC 25923) and *Escherichia coli* (ATCC 25922) are one of the most common pathogenic bacteria.

As shown in the figure, no trace of bacterial growth is seen around scaffolding containing nanoparticles up to a radius of wound dress and this shows the antibacterial effect of  $\text{TiO}_2$  and  $\text{ZnO}$  nanoparticles. The results showed that the growth of gram-negative bacteria was more resistant to antibacterial nanoparticles. The reason for the greater resistance of gram-negative bacteria to nanoparticles can be attributed to the outer membrane, the structure of the bacterial wall, and the metabolism of this bacterium as shown in Figure 6.

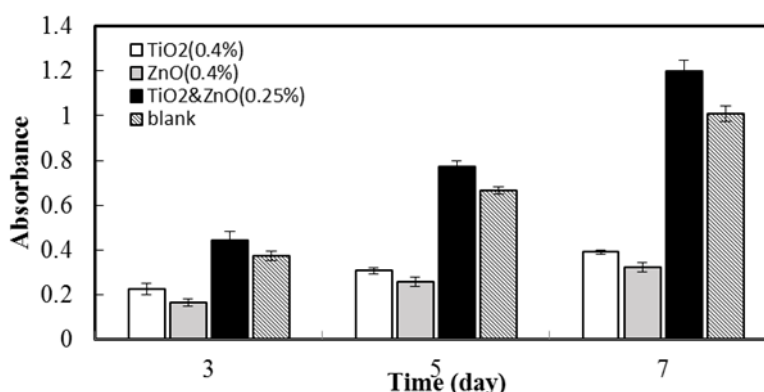
Figure 6 . Antibacterial effect of selected samples for gram-negative bacteria and gram-positive bacteria.



Cell viability assay

Figure 7 shows the growth characteristics of the cells in the 3rd, 5th, and 7th days. As shown in the figure, cell growth on scaffolding containing 2.5% nanoparticles is more than other scaffolds. As the results show, cell growth is good even on scaffolds without any nanoparticles, this in itself demonstrates the interaction and compatibility of the cell with the polymers used as shown in Figure 7.

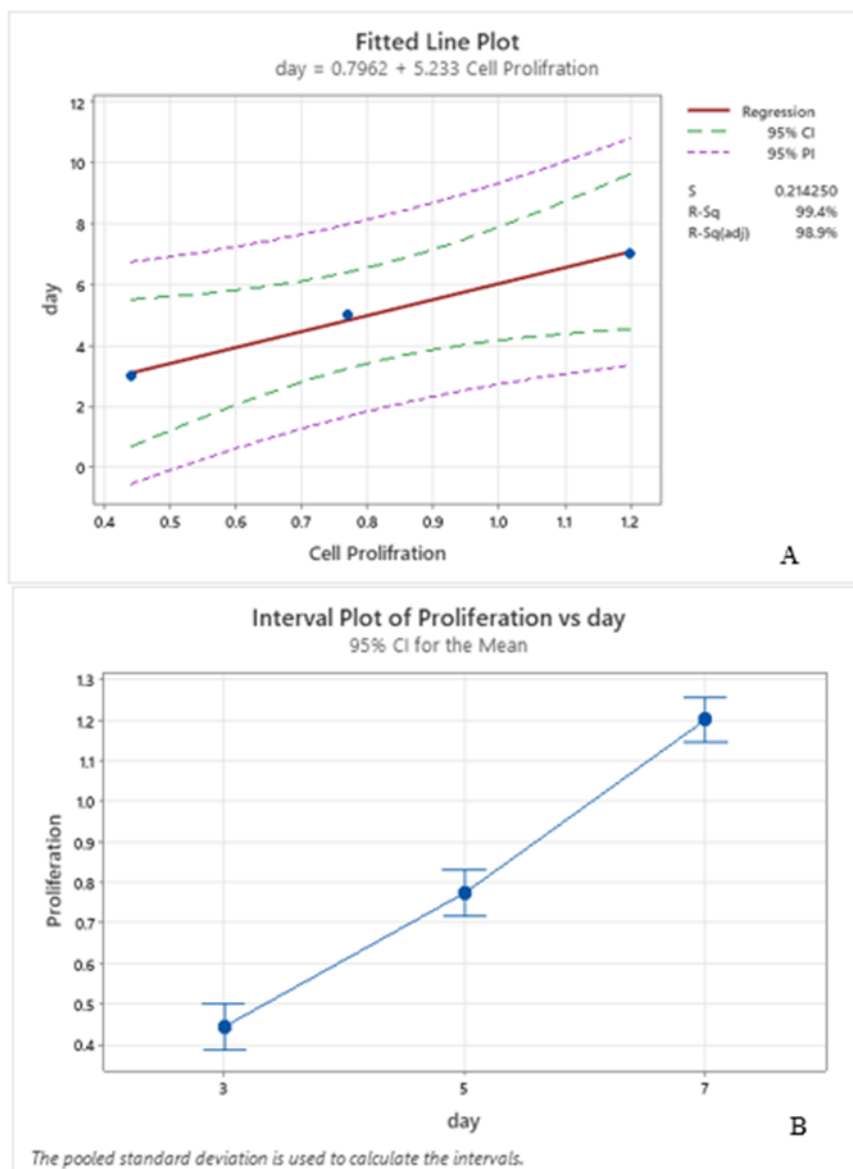
Figure 7. Shows cell growth on the third, fifth, and seventh days for samples with different nanoparticle percentages.



With the passing of time, the rate of cell growth in the scaffold increases, which indicates the capacity of the scaffold to improve cell growth with the time passing, which the Figure 8A shows well the linear relationship between cell proliferation and time. If the rate of cell growth is compared on the third, fifth and seventh days, according to the ANOVA as shown in Figure 8B: with P-value: 0.00 approves the increased rate in cell proliferation.

Based on the normal distribution function of the data, F method has been used to obtain the equal variance evaluation. According to the statistical analysis done by Minitab, the p value obtained from the one way ANOVA is equal to zero. The zero p-value indicates the growth and differentiation of cells in day 3, 5 and 7 as shown in Figure 8.

**Figure 8.** (A) show a linear relationship between cell proliferation and time (Day 3, 5 and 7) in sample TiO<sub>2</sub> and ZnO 2.5% and (B) shows cell proliferation in day 3, 5 and 7 in same sample. **Note:** ( — ) Regression; ( - - - ) 95% CI; ( - - - ) 95% PI.

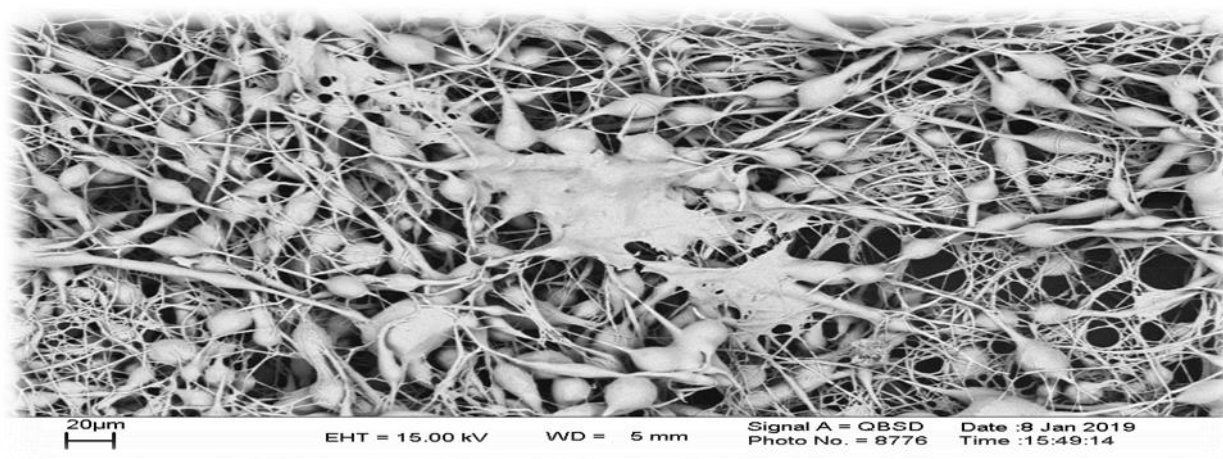


### Cell adhesion assay

Examination of cell adhesion on polymer fibers can be obtained from SEM images. Due to the use of polyhydroxy ethyl methacrylate in the preparation of nanofibers, a very suitable three-dimensional space is provided for the growth and adhesion of cells. In this polymer scaffold, a strong hydration barrier is created that prevents the absorption of protein, and as a result, the cells do not adhere completely to the surface, which is created due to the strong hydrogen bond between the water molecules and the polymer [28,29].

The images obtained from the scanning electron microscopy show the morphology of the cells stretched toward the scaffold. At present, it can be said that electrospun pHEMA- PCL nanofibers have good biocompatibility as shown in Figure 9.

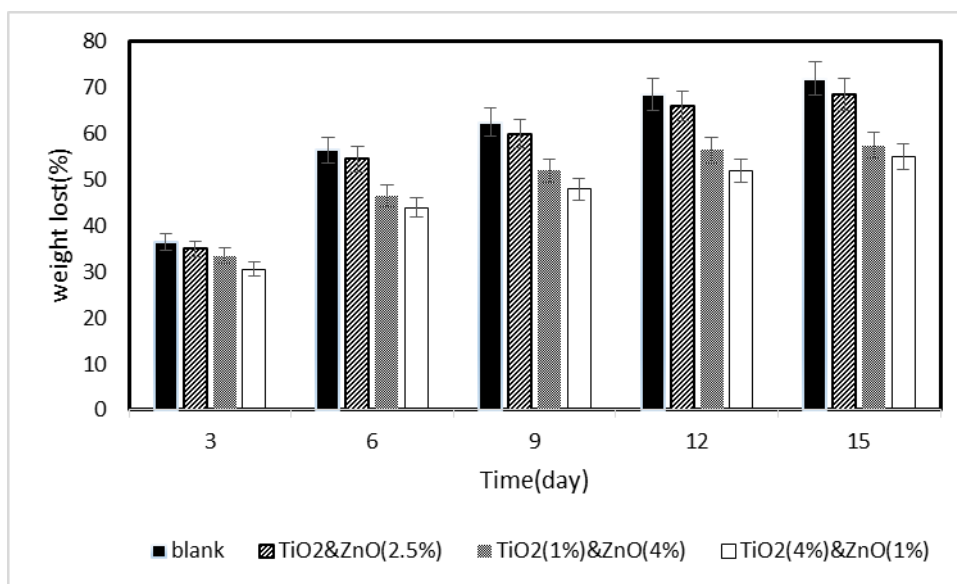
Figure 9. Shows the adhesion of the cell to the surface of the nanofibers that make up the scaffold.



### Bio-degradability assay

The results of the weight loss test in Figure 10 showed that the process of weight loss of scaffolding was done with great intensity until the 15th day, but after the 15th day, this process was done at a very low speed. The sample containing 0% of zinc oxide and titanium oxide nanoparticles showed more weight loss than other samples as shown in Figure 10.

Figure 10. Weight loss in day 3, 6, 9 12 and 15.



### CONCLUSION

Optimal scaffolding is a pattern for tissue regeneration and plays a key role in shaping the final structure of engineered tissue and its ultimate function. The most important step in tissue engineering is choosing the right materials and the right way to make scaffolding. They must have several essential characteristics such as biocompatibility, biodegradability, and biological activity. Achieving success in the performance of skin substitutes is specifically based on how the cell behaves and the growth of the tissue, in which case it is necessary to use a bio-

substance that can well provide the biological and mechanical properties of the skin tissue to provide nano topography to facilitate and modify cell exchanges with the environment, it is appropriate to provide nanoscale scaffolds, the production of which has attracted the attention of researchers in recent years. Different methods are used to prepare nanofibers, the most common of which are electrospinning, self-organizing, and fuzzy separation. Artificial polymers have mechanical properties superior to natural polymers and are easily processed. Polycaprolactone is a hydrophobic semi-crystalline polymer. Also, characteristics (C<sub>6</sub>H<sub>10</sub>O<sub>2</sub>) n Extraordinary mechanical molecular formula (mechanical flexibility), biocompatibility, it has low antigenicity, simple and easy processability, low melting point, and non-toxicity of the product resulting from its destruction. HEMA is a monomer used to make various polymers and is easily polymerized. HEMA and PCL nanofibers can support a wide range of cell types. One of the disadvantages of using caprolactone polymer is water repellency and consequently improper cell attachment. However, by combining this polymer with HEMA, a three-dimensional structure is created in the scaffold, in which the cell grows well in this three-dimensional environment. Studies have shown that cultured fibroblasts multiply three-dimensional faster than two-dimensional cultures. These differences appear to be due to the proximity of the cell space in the three-dimensional culture (culture on scaffolding) to the living environment. The results of the survival test in this study showed that the cells that grew on the scaffold of polymeric composition showed more absorption compared to the cells cultured on the scaffold of polycaprolactone.

TiO<sub>2</sub> and ZnO loaded pHEMA-PCL scaffold via inexpensive electrospinning method was fabricated. Percentages of each nanoparticle, voltage, and the rate of electrospinning, affect the morphology of the scaffold. Any substance unique properties but a composite of these materials has acceptable features such as being antibacterial, non-toxic, biocompatibility, biodegradability, and porosity which have all the properties of a suitable scaffold.

This scaffold contains 80% PCL, 15% HEMA, 2.5% TiO<sub>2</sub> and 2.5% ZnO Different percentages of NPS have been examined in this experiment but the growth and proliferation of fibroblast cells showed that the 2.5% of each nanoparticle is the best composition.

The antibacterial effect of nanoparticles was investigated and the result was satisfying. Because of mentioned features, this scaffold can be used as a wound dress and skin tissue scaffold.

### ACKNOWLEDGEMENT

The authors declare that they have no known competing financial interests or personal relationships that could have appeared to influence the work reported in this paper. Also the authors thank Professor Ali Baradar Khoshfetrat (Sahand University of Technology, Tabriz, Iran) for his technical assistance. This study was kindly supported by Iranian Council of Stem Cell Technology (No. 2022-016).

### REFERENCES

1. Díaz-Prado S, et al. Human amniotic membrane as an alternative source of stem cells for regenerative medicine. *Differentiation*. 2011;81:162-171.
2. Torres E, et al. Development and characterization of polyester and acrylate-based composites with hydroxyapatite and halloysite nanotubes for medical applications. *Polymers*, 2020;12:1703.



3. Gomez JA, et al. Study on stress evolution in the cooling process of micro hot embossing. *J. Mater. Sci.* 2014;9:20.
4. Rohit KV, et al. Zinc oxide (ZnO) nanoparticles: Synthesis properties and their forensic applications in latent fingerprints development. *Materials Today: Proceeding.* 2022;69:36-41.
5. Huang Z, et al. Bactericidal mode of titanium dioxide photocatalysis. *J. Photochem. Photobiol. A: Chem.* 2000;130:163-170.
6. Pham QP, et al. Electrospinning of polymeric nanofibers for tissue engineering applications: a review. *Tissue Eng.* 2006;12:1197-1211.
7. Wu T, et al. Resorbable polymer electrospun nanofibers: History, shapes and application for tissue engineering. *Chin. Chem. Lett.* 2020;31:617-625.
8. Cavaliere S, et al. Electrospinning: designed architectures for energy conversion and storage devices. *Energy Environ. Sci.* 2011; 4:4761-4785.
9. Gopal R, et al. Electrospun nanofibrous filtration membrane. *J. Membr. Sci.* 2006;281:581-586.
10. Duan G, et al. Exploration of macroporous polymeric sponges as drug carriers. *Biomacromolecules.* 2017;18:3215-3221.
11. Ryu H, et al. Uniform-thickness electrospun nanofiber mat production system based on real-time thickness measurement. *Sci. Rep.* 2020;10:1-10.
12. Zhang CL, et al. Nanoparticles meet electrospinning: recent advances and future prospects. *Chem Soc Rev.* 2014;43:4423-4448.
13. Solmaz Z, et al. Osteogenesis promotion of selenium-doped hydroxyapatite for application as bone scaffold. *Biol Trace Elem Res.* 2021;199:1802-1811.
14. Ren L, et al. Highly efficient fabrication of polymer nanofiber assembly by centrifugal jet spinning: process and characterization. *Macromol.* 2015;48:2593-2602.
15. Sridhar R, et al. Electrospayed nanoparticles and electrospun nanofibers based on natural materials: applications in tissue regeneration, drug delivery and pharmaceuticals. *Chem Soc Rev.* 2015;44(3), 790-814.
16. Beachley V, et al. Effect of electrospinning parameters on the nanofiber diameter and length. *Mater Sci Eng C.* 2009;29:663-668.
17. de Bartolo L, et al. Biomaterials for stem cell therapy: State of art and vision for the future. 2013.
18. Kikuchi A, et al. Nanostructured designs of biomedical materials: applications of cell sheet engineering to functional regenerative tissues and organs. *J Control Release.* 2005;101:69-84.
19. Ito E, et al. Active platelet movements on hydrophobic/hydrophilic microdomain-structured surfaces. *J Biomed Mater Res.* 1998;42:148-155.
20. Nojiri C, et al. *In vivo* protein adsorption on polymers: Visualization of adsorbed proteins on vascular implants in dogs. *J Biomater Sci Polym Ed.* 1993;4(2):75-88.
21. Robert S. 2016 Guidelines of the American Society of Mammalogists for the use of wild mammals in research and education. *J Mammal.* 2016;97:663-688.
22. Griffin JL, et al. Standard reporting requirements for biological samples in metabolomics experiments: mammalian/in vivo experiments. *Metabolomics.* 2007;3:179-188.

23. Fares MM, et al. Smart pH-sensitive alternating copolymers of (methylacrylamide-hydroxyethylmethacrylate); kinetic and physical properties. *J. Macromol. Sci. Part A.* 2009;47:61-70.
24. Gatti S, et al. Synthesis and nanoprecipitation of HEMA-CLn based polymers for the production of biodegradable nanoparticles. *Polymers.* 2017;9:389.
25. del Ángel-Sánchez K, et al. Development, fabrication, and characterization of composite polycaprolactone membranes reinforced with TiO<sub>2</sub> nanoparticles. *Polymers.* 2019;11:1955.
26. refi MR, et al. Synthesis of zinc oxide nanoparticles and their effect on the compressive strength and setting time of self-compacted concrete paste as cementitious composites. *Int J Mol Sci.* 2012;13:4340-4350.
27. Causa F, et al. Surface investigation on biomimetic materials to control cell adhesion: the case of RGD conjugation on PCL. *Langmuir.* 2010;26:9875-9884.
28. Prime KL, et al. Self-assembled organic monolayers: model systems for studying adsorption of proteins at surfaces. *Science.* 1991;1164-1167.
29. Shahverdi M, et al. Melt electrowriting of PLA, PCL, and composite PLA/PCL scaffolds for tissue engineering application. *Scientific Reports.* 2022;12:19935.